Ultrastructural Characteristics of Axons in Traumatic Neuromas of the Human Lingual Nerve

Amit R. Vora, PhD, BMedSci, BDS
Research Associate

Alison R. Loescher, PhD, MBChB, BDS, FDSRCS
Senior Lecturer in Oral and Maxillofacial Surgery

Fiona M. Boissonade, PhD, BDS
Professor of Oral Neuroscience

Peter P. Robinson, PhD, DSc, BDS, FDSRCS, FMedSci
Professor of Oral and Maxillofacial Surgery

Department of Oral and Maxillofacial Surgery
University of Sheffield
Sheffield, United Kingdom

Correspondence to:
Dr Alison R. Loescher
Department of Oral and Maxillofacial Surgery
School of Clinical Dentistry
University of Sheffield
Claremont Crescent
Sheffield S10 2TA
United Kingdom
Fax: +44 114 271 7863
E-mail: A.Loescher@sheffield.ac.uk

Aims: *To determine the ultrastructural characteristics of axons in traumatic neuromas of the human lingual nerve during the surgical removal of lower third molar teeth and to establish whether any characteristics were different between patients with dysesthesia and patients without dysesthesia.* ***Methods:*** *Transmission electron microscopy was used to determine the ultrastructural morphological characteristics of human lingual nerve neuromas (n = 34) removed at the time of microsurgical nerve repair. From a sample population of myelinated and nonmyelinated fibers within the neuromas, fiber diameter, myelin thickness, g-ratio, and the number of mitochondria per axon were quantified. Comparisons were made with normal control lingual nerve specimens (n = 8) removed at the time of organ donor retrieval.* ***Results:*** *Significant differences in ultrastructural morphology were found between the neuromas and control nerves. The neuromas contained a higher proportion of small (2- to 8-μm diameter) myelinated nerve fibers than controls, and the mean myelinated fiber diameter was significantly lower in neuromas than in controls. Mean myelin sheath thickness was significantly thinner in neuromas (0.6 ± 0.1 μm) than in controls. However, the g-ratio, which is a measure of the myelination status of the nerve fibers in relation to their diameter, was found to be similar in each group, suggesting a normal process of myelination in the damaged axons. Nonmyelinated axon diameter was also significantly smaller in the neuromas than in the controls, and Schwann cells were found to sheathe more nonmyelinated axons in neuromas than in controls. The ratio of nonmyelinated to myelinated axons was significantly higher in neuromas than in controls. However, no significant differences were found between patients with dysesthesia and those without dysesthesia.* ***Conclusion:*** *Damage to the lingual nerve results in marked changes to axon diameter, myelin sheath thickness, and Schwann cell-axon relationships. These ultrastructural changes could contribute to the altered electrophysiological properties of axons trapped within neuromas. However, no significant differences in the ultrastructural characteristics studied were found between specimens from patients with or without symptoms of dysesthesia.*
J OROFAC PAIN 2005;19:22–33

Key words: dysesthesia, human lingual nerve, traumatic neuromas

The development of the chronic painful sensory disorder of dysesthesia after peripheral nerve injury represents a substantial clinical problem, as it is a very difficult condition to treat.[1,2] The mechanisms underlying this disorder are not well understood; both central and peripheral mechanisms are implicated.[3–5] The current investigation was focused on the potential mechanisms that could be involved at the injury site, where a traumatic neuroma can develop.[3] Previous studies have shown that

afferent fibers trapped within a neuroma may develop spontaneous activity, and altered mechanosensitivity and chemosensitivity,[6–9] which may account for the initiation of the abnormal sensations experienced by the patient. The objective of the present study was to identify ultrastructural characteristics that may contribute to this abnormal behavior.

Spontaneous ectopic activity can occur within a few days of sectioning a peripheral nerve. Initially this occurs within the myelinated fibers, with C-fibers becoming spontaneously active later.[9–12] Peak ectopic activity is seen between 3 days and 3 weeks after injury,[12–15] and spontaneous activity can persist for several months. For example, Meyer et al found that 7 months after injury to the superficial radial nerve in baboons, 18% of fibers were still spontaneously active, and the rate of firing was greater in nonmyelinated C-fibers than in myelinated fibers.[7] Fried and Frisén[9] have suggested that this activity may be related to the presence of large endbulbs which develop on the damaged axons. These have been described as being club-shaped swellings, 3 to 12 μm in diameter, with dense accumulations of membrane-bound and cytoplasmic organelles.[16]

Other changes are also seen at the injury site. A preferential loss of large myelinated axons has been documented in several experimental models of neuroma formation and neuropathic pain states.[17–19] The loss of these large-diameter (Aβ) primary afferents and the subsequent loss of central inhibitory controls could allow for the disinhibition of the smaller pain-transmitting Aδ- and C-fibers. This idea is consistent with the Gate Control theory of pain transmission.[20] In support of this, painful human neuromas have been shown to contain higher than normal proportions of small nonmyelinated fibers.[21]

The present investigation concerns the lingual nerve, which is a branch of the mandibular division of the trigeminal nerve. The anatomical location of the lingual nerve in the mandibular third molar region makes it vulnerable to injury during oral and maxillofacial surgery.[22–24] The removal of impacted lower third molar teeth is a frequently performed operation, and the reported incidence of lingual nerve damage during this procedure ranges from 0.5% to 23%.[25–28] Afferent fibers in the lingual nerve innervate the mucous membranes of the floor of the mouth, the lingual gingivae, and the anterior two thirds of the tongue.[29–31] The nerve also carries visceral efferent (secretomotor) fibers to the submandibular and sublingual salivary glands, and special afferent (taste) fibers from the mucous membrane of the tongue, which are relayed via the chorda tympani branch of the facial (VII) nerve. Thus, injury to the lingual nerve results in ipsilateral sensory loss from the region described, including loss of taste sensation from the ipsilateral fungiform papillae.[32] The majority of patients who suffer damage to this nerve regain normal sensation within 9 to 12 months, but a small group (approximately 0.5% to 1%) are left with permanent sensory disturbances, such as dysesthesia.[33,34]

An extensive archive of traumatic neuroma specimens, together with clinical histories, from patients undergoing microsurgical repair of their damaged lingual nerves, was collected. The aims of the study were to use electron microscopy to determine the ultrastructural characteristics of axons in traumatic neuromas that resulted from damage to the human lingual nerve during the surgical removal of lower third molar teeth and to establish whether any characteristics were different between patients with dysesthesia and patients without dysesthesia in the distribution of the damaged nerve. To the authors' knowledge, this study is the first to detail the ultrastructural characteristics of a large series of traumatic neuromas from patients and relate such findings to clinical symptoms. Other investigations into the characteristics of the specimens have been undertaken using light microscopic and immunohistochemical techniques. Preliminary results from these studies have been published in abstract form.[35–37]

Materials and Methods

Tissue Specimens

Traumatic neuroma specimens were examined from 34 patients (mean age 30.8 ± 7.9 years; range 18 to 54 years) who had undergone microsurgical repair of their damaged lingual nerves. The timing of the nerve repair was on average 16.5 ± 13.4 months following the initial nerve injury (range 0.75 to 65 months). The microsurgical procedure has been described in detail by Robinson et al,[2] and the segment excised prior to repair ranged from 4 to 14 mm in length.

The specimens were characterized as follows:

- Neuromas-in-continuity (NICs), n = 18. This term was used to describe a neuroma found to be bridging together the proximal and distal segments of the damaged nerve.

- Nerve-end neuromas (NENs), n = 16. In these cases, the nerve had been completely divided and the ends had separated, resulting in a nerve-end swelling on the central stump.

Portions of lingual nerve were taken from 8 patients immediately post mortem following the harvesting of their organs for transplantation purposes (mean age 40.3 ± 12.4 years; range 25 to 54 years). The specimens were obtained by elevating a lingual mucoperiosteal flap and excising a segment of nerve adjacent to the lower third molar area. These specimens served as the controls.

Ethical Approval

Ethical approval for the study was obtained from the South Sheffield Research Ethics Committee. Consent was obtained from the organ donors' next of kin to permit lingual nerve tissue to be obtained for research use.

Fixation and Processing

Immediately after harvesting the specimen, a transverse segment of 1 to 2 mm in thickness was taken from the central end of the neuroma (or an equivalent site in the control specimens) and immersion-fixed in 3% glutaraldehyde in 0.1 mol/L phosphate buffer overnight at 4°C. The specimens underwent secondary fixation in 1% aqueous osmium tetroxide at room temperature for 90 minutes and were then dehydrated through a series of alcohols prior to embedding in Agar 100 epoxy resin (Agar Scientific). Ultrathin sections (80 to 90 nm) were cut, collected on Formvar-coated 50-mesh copper tabbed grids (Agar Scientific), and stained using saturated uranyl acetate in 50% methanol and lead citrate solution.

Sampling Methodology

Because of the size of the neuroma specimens (up to 4 mm in diameter), a randomized systematic sampling plan was devised in accordance with the protocols suggested by Mayhew[38] and Mayhew and Sharma.[39] Low-power electron microscopic scans of each grid square containing nerve tissue were taken at 740× magnification with a Phillips CM10 transmission electron microscope. A suitably sized counting frame for each grid square corner was chosen from the images obtained so that approximately 200 myelinated fibers per specimen could be analyzed in detail at a magnification of 10,500× using a Zeiss EM 109 transmission electron microscope. Prints were produced from the electron micrographs using a dedicated film scanner (Dîmage ScanMulti; Minolta) connected to a computer and printer. The prints were montaged, and the same area was subsequently reanalyzed under the electron microscope for nonmyelinated fibers, which were photographed and printed at a final magnification of 35,700×.

Myelinated and nonmyelinated fibers were measured with a digitizing tablet (Calcomp Drawing Board III, GTCOCalcomp) and Bioquant System IV image analysis software (R&M Biometrics). The following characteristics were determined: axon diameter, myelinated fiber diameter, g-ratio (a measure of the myelination status of the nerve fibers in relation to their diameter), myelin sheath thickness, and the number of mitochondria per axon.

Diameter values were calculated from measurements of circumference divided by π, since circumference values are relatively unaffected by alterations in buffer molarity, unlike fiber shape or area.[40] This diameter value, therefore, is based upon the assumption that the transverse profiles of the fibers measured were circular. Fibers that were sectioned obliquely were thus excluded from sampling. They were defined as those fibers having a diameter in one direction measuring at least twice that in another.[41]

Myelin sheath thickness was also calculated from the formula described by Holland[40]:

$$\text{Myelin sheath thickness} = \frac{\text{External circumference} - \text{Internal circumference}}{2\pi}$$

The g-ratio was determined as another measurement of myelination. The g-ratio is the ratio between the axon diameter (inner diameter) divided by the total myelinated fiber diameter.[42,43]

All the specimens were coded, and analysis was performed by the same examiner, who was blind to the patient's symptomology.

Clinical Histories

The clinical histories and symptoms of the patients undergoing microsurgical repair of their damaged lingual nerves were obtained prospectively using a questionnaire. All the patients undergoing surgery had marked sensory loss, with variable degrees of dysesthesia. Patients were asked whether the affected part of the tongue was painful and whether they had tingling (paresthesia) that was spontaneous or initiated by touching or moving the tongue. In addition, a series of sensory tests

was performed; these are described in detail by Robinson et al.[2] Some patients also scored their pain and tingling symptoms on visual analog scales. For the purposes of this study, to allow for statistical comparisons, patients were classified into 2 groups:

- No-symptoms group: Those experiencing no pain or tingling
- Symptoms group: Those experiencing either pain or tingling that was spontaneous or initiated by touching or moving the tongue.

Pain or tingling elicited by firm digital palpation over the neuroma was present in most patients and therefore was not used as a criterion for entry into the latter group. There were no significant differences between the 2 groups with regard to age, sex distribution, or length of time between the injury and the repair.

Statistical Analysis

Statistical comparisons (1-way analysis of variance [ANOVA] and Tukey-Kramer multiple comparison tests) were made between the neuroma and control groups, and between patients with and without symptoms, for each of the ultrastructural characteristics. Simple linear regression was performed to determine whether any relationship existed between the time after nerve injury and any ultrastructural features within neuromas. A P value of less than .05 was selected as the criterion of significance.

Results

A total of 8,333 myelinated axons (mean ± SD, 198 ± 118 fibers per specimen; range 30 to 611) and 19,699 nonmyelinated axons (469 ± 316 fibers per specimen, range 91 to 1,259) were analyzed.

Ultrastructural Characteristics of Myelinated Axons

Mean myelinated fiber diameter was significantly smaller in traumatic neuromas than in control nerves (ANOVA, $P < .001$) (Fig 1). In control nerves, the mean myelinated fiber diameter was 6.3 ± 0.6 μm, compared to 4.3 ± 0.8 μm in NICs and 3.9 ± 0.5 μm in NENs. No significant difference in fiber diameter was found between the NICs and the NENs, nor between patients with or without symptoms (Table 1). A comparison between the mean myelinated fiber diameter and time after injury failed to reveal any significant correlation ($P > .3$).

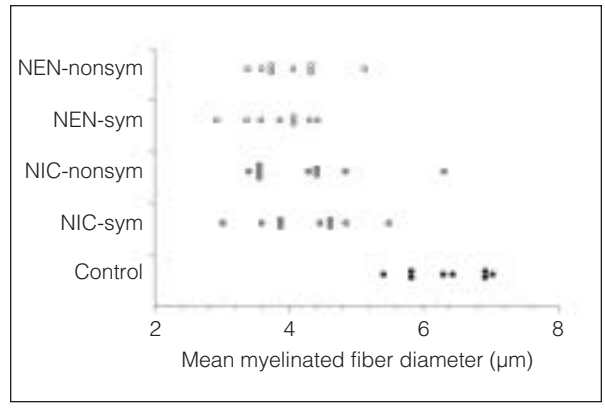

Fig 1 Spread plot showing the mean myelinated fiber diameter in control nerves, NENs, and NICs from patients with symptoms (sym) and without symptoms (nonsym). Mean myelinated fiber diameter was significantly smaller in NENs and NICs than in controls. (ANOVA, $P < .001$).

Figure 2 shows pooled histogram data for myelinated nerve fiber diameter in control nerves, NICs, and NENs. Traumatic neuromas were found to contain a higher proportion of small myelinated nerve fibers with diameters of 2 to 8 μm (NICs: 92.3%; NENs: 93.1%) than control nerves (76.1%). Figure 3 shows examples of the ultrastructural appearance of myelinated nerve fibers in a control nerve and a traumatic neuroma.

The myelin sheaths were found to be significantly thinner in myelinated axons in traumatic neuromas than in those in controls (ANOVA, $P < .001$) (Fig 4a). Mean myelin sheath thickness was 1.1 ± 0.1 μm in control nerves versus 0.6 ± 0.1 μm in both NICs and NENs. However, no significant difference in myelin sheath thickness was found between patients with symptoms and those without symptoms (Table 1). Despite mean myelin thickness being significantly different, the mean g-ratio (axon diameter/myelinated fiber diameter) was found to be similar ($P = .07$) in controls (0.66 ± 0.01), NICs (0.69 ± 0.04), and NENs (0.71 ± 0.05) (Fig 4). In addition, there was no difference in mean g-ratio between patients with symptoms and those without symptoms (Table 1).

No significant difference was observed in the mean number of mitochondria per myelinated axon between the various groups (controls: 5.6 ± 1.3; NICs: 5.0 ± 0.9; NENs: 4.9 ± 0.6; $P = .4$), nor between patients with and without symptoms (Table 1).

Table 1 Comparison of Ultrastructural Characteristics of Myelinated Axons in NICs and NENs in Patients with Symptoms and Patients Without Symptoms

	NICs			NENs		
	Symptoms	No symptoms	*P*	Symptoms	No symptoms	*P*
Myelinated fiber diameter (μm)	4.3 ± 0.7	4.3 ± 0.9	> .99	3.8 ± 0.5	4.0 ± 0.6	.97
Myelin sheath thickness (μm)	0.6 ± 0.2	0.7 ± 0.1	.97	0.6 ± 0.06	0.6 ± 0.02	.99
G-ratio	0.70 ± 0.04	0.67 ± 0.04	.54	0.70 ± 0.04	0.71 ± 0.06	.95
No. of mitochondria per myelinated axon	4.8 ± 1.0	5.2 ± 0.8	.91	4.9 ± 0.6	4.9 ± 0.7	> .99

Means ± standard deviations shown; *P* values obtained with Tukey-Kramer multiple comparisons test.

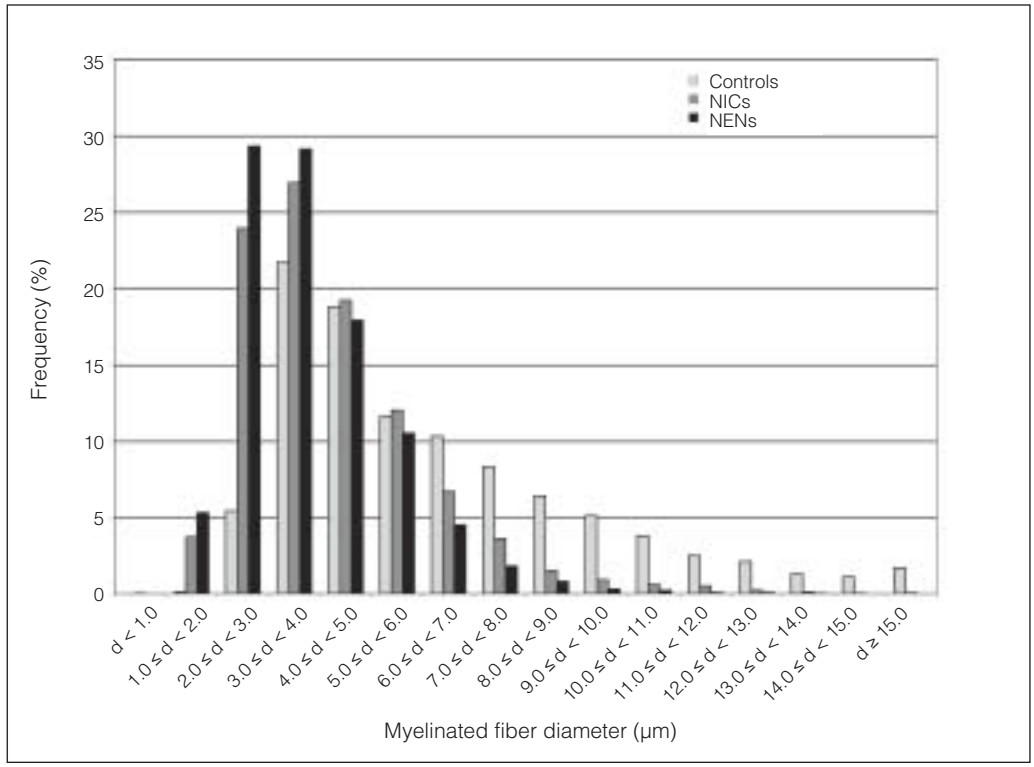

Fig 2 Pooled histogram data for myelinated fiber diameter in control nerves, NICs, and NENs. d = diameter.

Ultrastructural Features of Nonmyelinated Axons

The mean nonmyelinated axon diameter was significantly larger in controls than in traumatic neuromas (ANOVA, $P < .001$). Mean nonmyelinated axon diameter was 1.03 ± 0.13 μm in controls, compared to 0.67 ± 0.13 μm in NICs and 0.58 ± 0.13 μm in NENs. There was also a significant difference between the NENs and NICs (ANOVA, $P < .05$) (Fig 5). However, no significant differences were found between patients with or without symptoms (Table 2). In addition, no correlation was found between axon diameter and time after nerve injury ($P > .25$).

Figure 6 shows pooled histogram data for nonmyelinated fiber diameter. The traumatic neuroma specimens contained a higher proportion of small axons of 0.25 to 0.75 μm diameter (NICs: 62.4%; NENs: 68.4%) compared to normal lingual nerves (33.6%).

Significant differences were also observed between neuromas and controls in the number of nonmyelinated axons sheathed by a Schwann cell in each Remak bundle. Traumatic neuromas contained more nonmyelinated axons per Remak bundle than controls, and examples of the ultrastructural appearance of the axon-Schwann cell relationship are shown in Fig 7. Control nerves

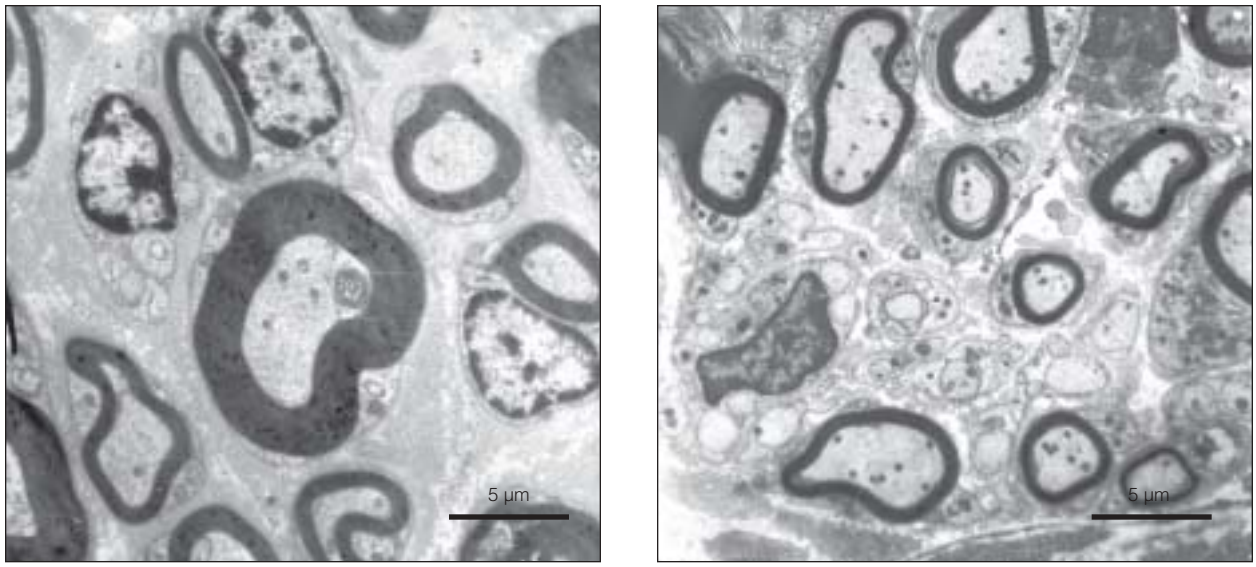

Fig 3 Myelinated and nonmyelinated axons in *(left)* a control lingual nerve and *(right)* a traumatic neuroma.

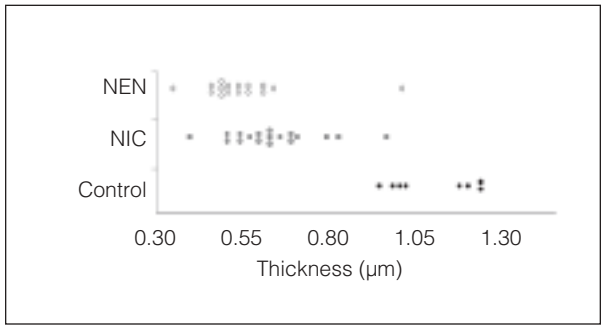

Fig 4a Spread plot showing mean myelin thickness (in µm) in NENs, NICs, and controls. The myelin sheaths were found to be significantly thinner in myelinated axons in NENs and NICs than in those in controls (ANOVA, $P < .001$).

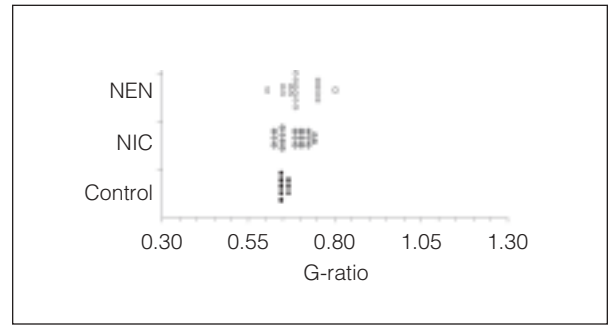

Fig 4b Spread plot showing mean g-ratio in NENs, NICs, and controls.

were found to contain an average of 2.0 ± 0.4 axons/Schwann cell, compared to 2.9 ± 0.7 in NICs and 3.1 ± 1.1 in NENs (ANOVA, $P < .05$). No significant difference was found in the mean number of axons/Schwann cell between the NENs and NICs or between patients with symptoms and those without symptoms (Table 2). No correlation was found between the number of axons/Schwann cell bundle and time after injury ($P > .5$).

A significant difference was observed in the mean number of mitochondria per nonmyelinated axon, with higher counts being present in axons within the NENs (5.3 ± 0.6) compared to NICs (4.0 ± 0.9) and controls (4.4 ± 1.2; ANOVA, $P < .005$) (Fig 8). However, no significant difference was observed between patients with symptoms and those without symptoms (Table 2).

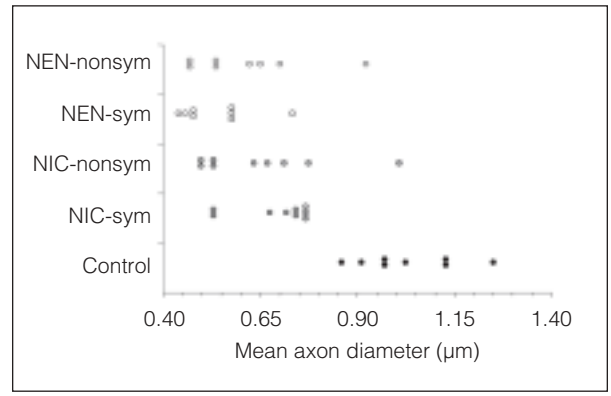

Fig 5 Spread plot showing the mean nonmyelinated axon diameter in control nerves, NICs, and NENs from patients with symptoms (sym) and without symptoms (nonsym). Mean nonmyelinated axon diameter was significantly larger in controls than in traumatic neuromas (ANOVA, $P < .001$). There was also a significant difference between the NENs and NICS (ANOVA, $P < .05$).

Table 2 Comparison of Ultrastructural Characteristics of Nonmyelinated Axons in NICs and NENs in Patients with Symptoms and Patients Without Symptoms

	NICs			NENs		
	Symptoms	No symptoms	*P*	Symptoms	No symptoms	*P*
Nonmyelinated axon diameter (μm)	0.69 ± 0.10	0.65 ± 0.17	.96	0.54 ± 0.10	0.57 ± 0.20	.83
No. of axons per Schwann cell bundle	2.8 ± 0.60	3.0 ± 0.90	.99	2.8 ± 0.80	3.4 ± 1.31	.60
No. of mitochondria per nonmyelinated axon	3.8 ± 1.2	4.3 ± 0.5	.87	5.2 ± 0.6	5.4 ± 0.6	.99
Ratio of nonmyelinated to myelinated axons in sampled area	2.6 ± 1.2	2.0 ± 0.9	.93	2.7 ± 1.2	4.3 ± 2.6	.24

Means ± standard deviations shown; *P* values obtained with Tukey-Kramer multiple comparisons test.

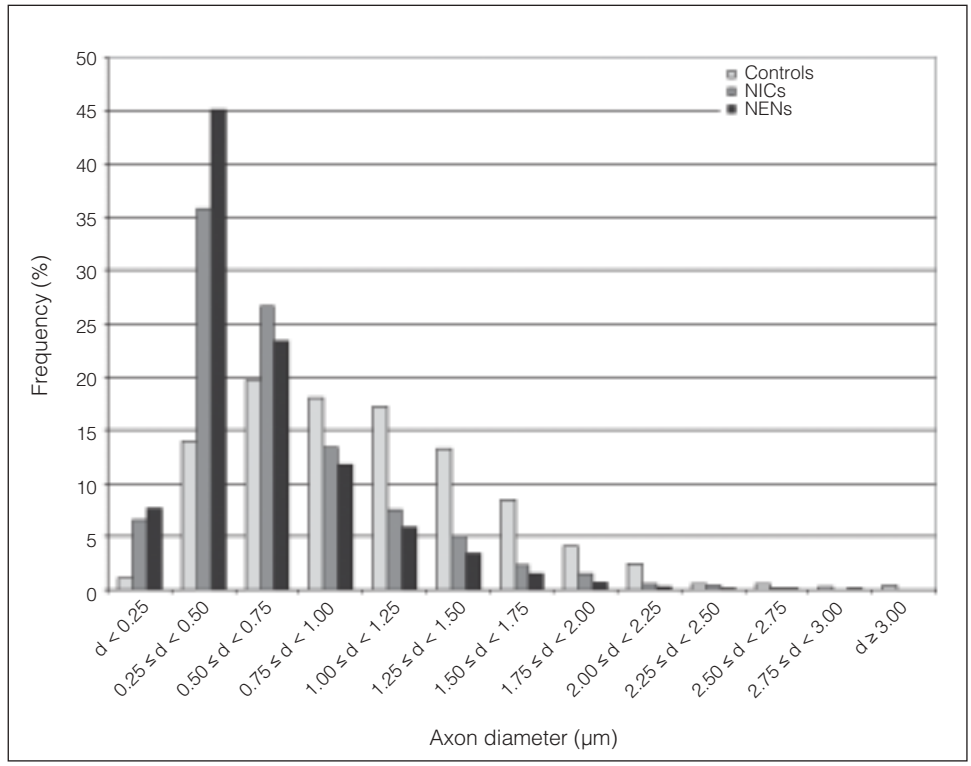

Fig 6 Histogram showing pooled data for nonmyelinated fiber diameter in control nerves, NICs, and NENs. d = diameter.

Ratio of Nonmyelinated to Myelinated Axons

The ratio of nonmyelinated axons to myelinated axons in the sampled area was significantly higher in traumatic neuromas than in the controls (ANOVA, $P < .005$) (Fig 9). In controls the ratio was 1.2 ± 0.3, compared to 2.3 ± 1.1 in NICs and 3.5 ± 2.1 in NENs. The difference in ratio between NENs and NICs was also significant (ANOVA, $P < .05$), but no significant differences were found between patients with or without symptoms (Table 2).

Discussion

There have been few previous quantitative structural studies on human lingual nerves. However, the range of myelinated nerve fiber diameters found in the control lingual nerves was similar to the findings of Heasman and Beynon[30] who studied post mortem specimens of lingual nerve from 20 human cadavers and found fiber diameters of 2 to 14 μm. The authors postulated that the fibers in the 2- to 4-μm range represented the myelinated Aδ

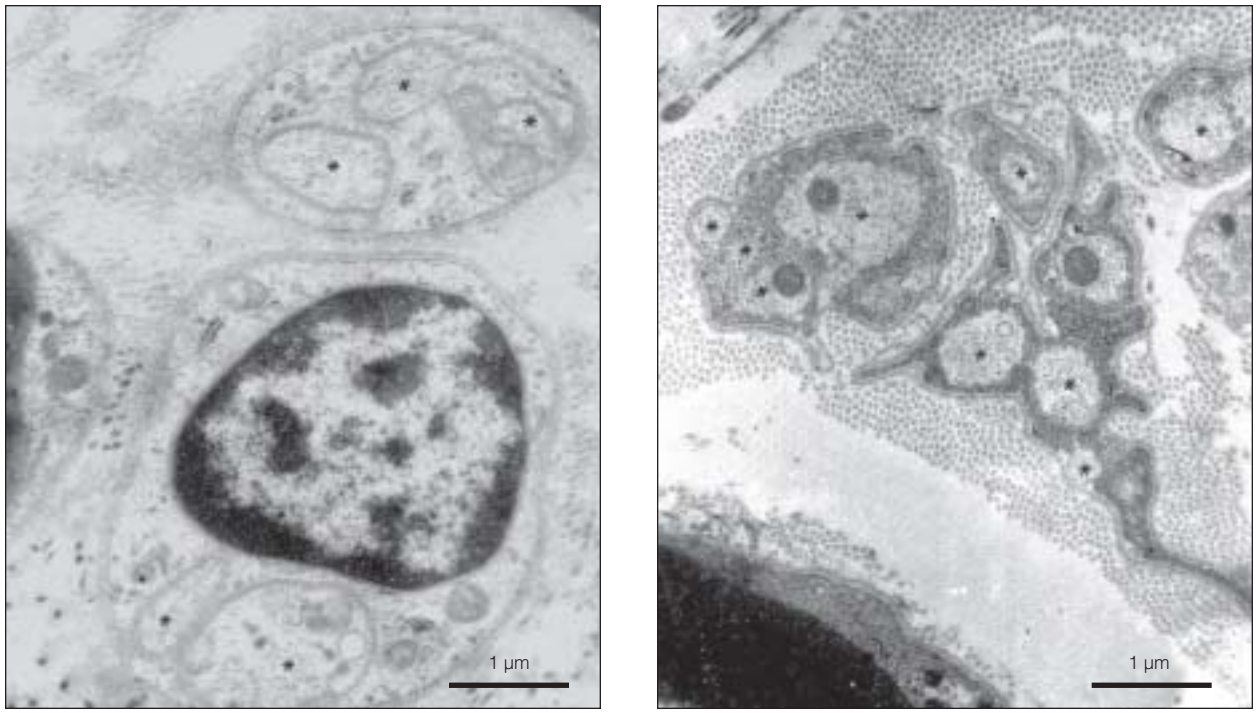

Fig 7 Nonmyelinated axons *(asterisks)* and their associated Schwann cells within *(left)* a normal lingual nerve and *(right)* a traumatic neuroma.

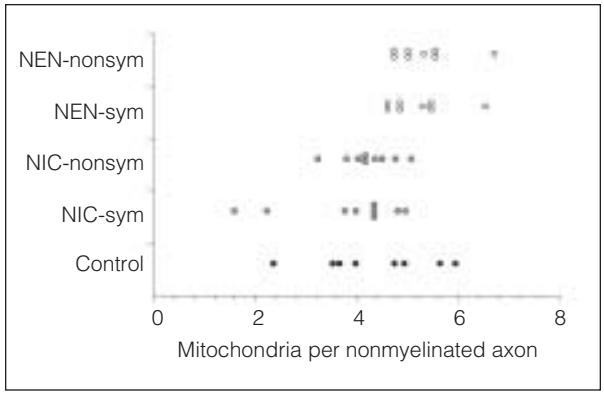

Fig 8 Spread plot showing the mean number of mitochondria per nonmyelinated axon diameter in control nerves, NICs, and NENs from patients with symptoms (sym) and without symptoms (nonsym). Significantly more mitochondria were found in the axons of the NENs than NICs and controls (ANOVA, $P < .005$).

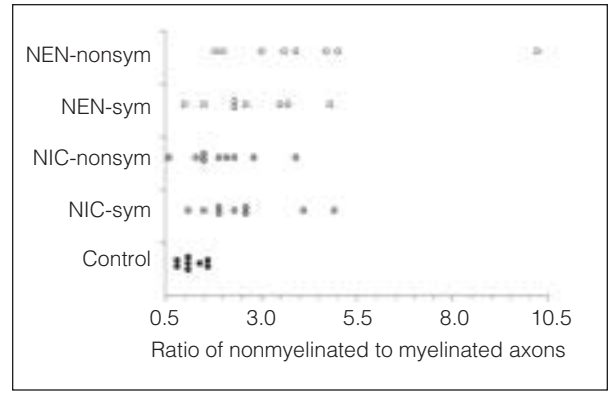

Fig 9 Spread plot showing the ratio between the number of nonmyelinated and myelinated axons in control nerves, NICs, and NENs from patients with symptoms (sym) and without symptoms (nonsym). The ratio of nonmyelinated axons to myelinated axons in the sampled area was significantly higher in NENs and NICs than in controls (ANOVA, $P < .005$). The difference in ratio between NENs and NICs was also significant.

afferents and the preganglionic secretomotor and taste fibers derived from the chorda tympani nerve. They suggested that the larger diameter fibers represented the Aβ and Aα somatic afferents mediating touch, pressure, proprioception, and vibration, although the course taken by the proprioceptive fibers from the tongue is a subject of debate.[44]

The results of the present study have shown that both myelinated and nonmyelinated axons in lingual nerve neuromas have significantly altered morphology compared to normal control nerves, despite long recovery periods after the nerve injury. The diameter distribution of the myelinated fibers in the neuromas was found to be markedly different

from controls; a high proportion of small axons with diameters of 2 to 8 μm was found in neuromas. A preponderance of thin fibers could indicate a loss of thick fibers, a relative increase in regenerating thin fibers, or a combination of the two.[45] Alternatively, the change in distribution of fiber size could represent a failure of maturation of axons rather than a lack of development and regeneration of a class of large fibers.[46] Maturation of regenerating axons may be arrested if the axon sprouts fail to reach and reinnervate their peripheral targets.[47] In addition, the connective tissue around the damaged nerve also becomes scarred, and discontinuity of perineurial tissue and vessels and alterations in the endoneurial microenvironment occur; all of these are factors that may retard axon development and maturation.[20,46] The branching of regenerating axons may also accentuate the preponderance of thin fibers within a neuroma,[45] and these multiple sprouts may persist within the neuroma even when regeneration is complete and the axons have formed functional endings.[48]

Schröder[49] found that 6 to 24 months after trauma to the sciatic nerve in dogs, the diameters of the regenerating nerve fibers were reduced when compared with normal axons, and that the myelin sheaths of the regenerated nerve fibers remained thin. Schröder also observed that the conduction velocity of these regenerated nerve fibers was reduced when compared with controls. The g-ratio, an important determinant of internodal conduction time, is the ratio of axon diameter (d) divided by the total fiber diameter (D).[43] Rushton[50] stated that the energetically most efficient value for d/D is 0.6, and Schröder[49] suggested that the reduced conduction velocity recorded in regenerated nerve fibers is largely the result of a reduction in the myelin sheath thickness. In the present study, mean myelin sheath thickness was found to be significantly thinner in axons in neuromas than in controls, but the mean g-ratio was found to be similar. This suggests that a normal process of myelination is occurring within the regenerating nerve fibers, and that the reduced mean myelin sheath thickness merely reflects the greater proportion of small-diameter nerve fibers in neuromas. The failure to see any increase in myelin sheath thickness at longer time periods after injury also probably reflects the impeded maturation of axons trapped within neuromas.[20,46,47]

The reduction in diameter of nonmyelinated fibers in neuromas has also been described by others. Following crush, graft, or multiple crush injury of the sciatic nerve in mice, Giannini et al[46] found a reduction in nonmyelinated fiber size distal to the injury and fewer nonmyelinated axons per Schwann cell in the regenerating nerves. This latter observation is in contrast to the present findings and those of others who have reported multiple axons per Schwann cell unit, presumably as a result of axonal branching.[51,52] Aguayo et al[53] transected the anterior mesenteric nerve in rabbits and 13 weeks later found a higher proportion of smaller-diameter nonmyelinated axons than in controls, with a reduction of diameter and an increased number of nonmyelinated axons per Schwann cell. Once again, the failure to establish terminal connections, and hence the impeded maturation of axons, may account for the reduction of nonmyelinated axon diameter following nerve section. The increase in axon to Schwann cell ratio may result from the axonal sprouting occurring at a greater rate than the limited Schwann cell multiplication.[53]

The complete transection of the nerve in the NEN group is clearly a more severe injury than a partial nerve injury, where some continuity exists between the proximal and distal segments. After a partial nerve injury there is also the possibility that, as well as containing regenerating or recovering axons, some undamaged fibers from the nerve may still remain postinjury. The NIC specimens may represent partial nerve injuries or successful regeneration across the gap between the 2 nerve stumps. The failure of any axons to reach their peripheral targets and possibly higher levels of branching may explain why the NEN specimens had significantly smaller nonmyelinated fiber diameters compared to the NICs. In addition, the higher numbers of mitochondria per axon within the NENs compared to controls and NICs may reflect those fibers terminating within the neuroma, since an accumulation of organelles within the axoplasm has been found in nerve endings.[16]

Several authors have suggested that the nonmyelinated fibers within neuromas have an important influence on whether or not pain is experienced by the patient. Carlton et al[18] found that hyperalgesia was still produced in their experimental model of neuropathic pain when large numbers of myelinated fibers were lost. The authors suggested that the presence of nonmyelinated axons was important, since fewer of those fibers were lost. Mathews and Osterholm,[54] in their review of painful traumatic neuromas, stated that pain-conducting C-fibers are more resistant to ischemia than other neural elements and therefore survive and function within a relatively "avascular" neuroma and cause pain.[54] Cravioto and Battista[21] in their clinical and ultrastructural study of 3 cases of painful neuromas of the median, sciatic, and per-

oneal nerves, found that painful neuromas contained large numbers of small-diameter unmyelinated fibers in a much higher proportion than myelinated fibers (sometimes up to 20 times greater). The authors, therefore, suggested that the fine unmyelinated fibers may generate the pain of human neuromas.[21] In the present study, a significant increase in the ratio of nonmyelinated to myelinated fibers was evident in neuromas compared to controls. However, no significant correlation between this higher ratio and the patients' clinical symptoms was found.

The failure to see any correlation between the ultrastructural features and the time after injury is probably not surprising. The present study investigated the morphology of the neuromas removed after "late" surgical repair of the damaged nerve; in many cases, several months elapsed between repair surgery and the initial injury. We would expect most structural changes to have stabilized by this time. This is different from published reports of neuroma morphology from several animal studies, where neuroma formation and nerve regeneration was followed over days and weeks rather than months, and axon number and size did not stabilize.[16,46,52,53,55] In the animal studies, attempts have been made to relate ultrastructural findings to apparent pain-related behavior.[17–19,56,57] These studies have mainly focused on behavioral symptoms within the first few weeks of injury and have associated the loss of large myelinated fibers with the onset of hyperalgesia. The present study is unique in that ultrastructural features of human neuroma specimens were correlated with actual pain histories from the patients. However, no significant differences in ultrastructure were found between patients with symptoms of pain and/or tingling and those without symptoms. This may be because of the method of random sampling of the axons within the neuroma specimens, which could make it difficult to identify what may be a small number of axons with aberrant properties giving rise to the patient's symptoms. There is also the possibility that peripheral changes within the neuroma tissue may not be the primary site for initiation or maintenance of chronic neuropathic pain following nerve transection.

In summary, this paper has shown that significant differences exist in ultrastructural morphology of myelinated and nonmyelinated axons in traumatic neuromas when compared to normal lingual nerve. Although these ultrastructural changes may contribute to alterations in the electrophysiological properties of axons, no correlations between the ultrastructural characteristics and the patients' symptoms of dysesthesia were found. Further investigations are required to investigate whether the observed ultrastructural changes are associated with other alterations in neuromas, such as ion-channel expression and neuropeptide levels, which have also been implicated in the etiology of neuropathic pain.[5,58–61]

Acknowledgments

To David Thompson and John Proctor for their assistance with the electron microscopy. To Sarah Bodell, Kath Elliott, Katie Brook, and Jo Firth for their help in scanning and printing the electron micrographs. To Sue Siddall (Regional Renal Transplant Coordinator, Northern General Hospital) and the respective families concerned, for giving consent and allowing us to obtain control lingual nerve specimens from organ donor patients. This work was supported by a grant from Action Research.

References

1. Gregg JM. Studies of traumatic neuralgia in the maxillofacial region: Symptom complexes and response to microsurgery. J Oral Maxillofac Surg 1990;48:135–140.
2. Robinson PP, Loescher AR, Smith KG. A prospective, quantitative study on the clinical outcome of lingual nerve repair. Br J Oral Maxillofac Surg 2000;38:255–263.
3. Gregg JM. Studies of traumatic neuralgias in the maxillofacial region: Surgical pathology and neural mechanisms. J Oral Maxillofac Surg 1990;48:228–237.
4. Woolf CJ, Mannion RJ. Neuropathic pain: Aetiology, symptoms, mechanisms, and management. Lancet 1999;353:1959–1964.
5. Zimmermann M. Pathobiology of neuropathic pain. Eur J Pharmacol 2001;429:23–37.
6. Devor M. Nerve pathophysiology and mechanisms of pain in causalgia. J Auton Nerv Syst 1983;7:371–384.
7. Meyer RA, Raja SN, Campbell JN, Mackinnon SE, Dellon AL. Neural activity originating from a neuroma in the baboon. Brain Res 1985;325:255–260.
8. Lisney SJ, Devor M. Afterdischarge and interactions among fibers in damaged peripheral nerve in the rat. Brain Res 1987;415:122–136.
9. Fried K, Frisén J. End structure and neuropeptide immunoreactivity of axons in sciatic neuromas following nerve section in neonatal rats. Exp Neurol 1990;109:286–293.
10. Wall PD, Gutnick M. Properties of afferent nerve impulses originating from a neuroma. Nature 1974;248:740–743.
11. Blumberg H, Jänig W. Discharge pattern of afferent fibers from a neuroma. Pain 1984;20:335–353.
12. Bongenhielm U, Robinson PP. Spontaneous and mechanically evoked afferent activity originating from myelinated fibres in ferret inferior alveolar nerve neuromas. Pain 1996;67:399–406.
13. Govrin-Lippmann R, Devor M. Ongoing activity in severed nerves: Source and variation with time. Brain Res 1978;159:406–410.

14. Bongenhielm U, Robinson PP. Afferent activity from myelinated inferior alveolar nerve fibers in ferrets after constriction or section and regeneration. Pain 1998;74:123–132.
15. Yates JM, Smith KG, Robinson PP. Ectopic neural activity from myelinated afferent fibres in the lingual nerve of the ferret following three types of injury. Brain Res 2000; 874:37–47.
16. Fried K, Govrin-Lippmann R, Rosenthal F, Ellisman MH, Devor M. Ultrastructure of afferent axon endings in a neuroma. J Neurocytol 1991;20:682–701.
17. Basbaum AI, Gautron M, Jazat F, Mayes M, Guilbaud G. The spectrum of fiber loss in a model of neuropathic pain in the rat: An electron microscopic study. Pain 1991; 47:359–367.
18. Carlton SM, Dougherty PM, Pover CM, Coggeshall RE. Neuroma formation and numbers of axons in a rat model of experimental peripheral neuropathy. Neurosci Lett 1991;131:88–92.
19. Coggeshall RE, Dougherty PM, Pover CM, Carlton SM. Is large myelinated fiber loss associated with hyperalgesia in a model of experimental peripheral neuropathy in the rat? Pain 1993;52:233–242.
20. Castaldo JE, Ochoa JL. Mechanical injury of peripheral nerves. Fine structure and dysfunction. Clin Plast Surg 1984;11:9–16.
21. Cravioto H, Battista A. Clinical and ultrastructural study of painful neuroma. Neurosurgery 1981;8:181–190.
22. Kiesselbach JE, Chamberlain JG. Clinical and anatomic observations on the relationship of the lingual nerve to the mandibular third molar region. J Oral Maxillofac Surg 1984;42:565–567.
23. Pogrel MA, Renaut A, Schmidt B, Ammar A. The relationship of the lingual nerve to the mandibular third molar region: An anatomic study. J Oral Maxillofac Surg 1995;53:1178–1181.
24. Behnia H, Kheradvar A, Shahrokhi M. An anatomic study of the lingual nerve in the third molar region. J Oral Maxillofac Surg 2000;58:649–651.
25. Rood JP. Lingual split technique. Damage to inferior alveolar and lingual nerves during removal of impacted mandibular third molars. Br Dent J 1983;154:402–403.
26. Von Arx DP, Simpson MT. The effect of dexamethasone on neurapraxia following third molar surgery. Br J Oral Maxillofac Surg 1989;27:477–480.
27. Robinson PP. Nerve injuries resulting from the removal of impacted teeth. In: Andreasen J, Petersen JK, Laskin DM (eds). Textbook and Color Atlas of Tooth Impactions—Diagnosis, Treatment, Prevention. Copenhagen: Munksgaard, 1997:469–490.
28. Bataineh AB. Sensory nerve impairment following mandibular third molar surgery. J Oral Maxillofac Surg 2001;59:1012–1017.
29. Biedenbach MA, Beuerman RW, Brown AC. Graphic-digitizer analysis of axon spectra in ethmoidal and lingual branches of the trigeminal nerve. Cell Tissue Res 1975;157:341–352.
30. Heasman PA, Beynon AD. Quantitative diameter analysis of lingual nerve axons in man. J Dent Res 1986;65: 1016–1019.
31. Watanabe IS, Semprini M, de Moraes SR, de Souza RR. Diameter of axons in the lingual nerve of the mouse. A preliminary investigation. Braz Dent J 1996;7:87–90.
32. Holland GR, Robinson PP. Peripheral nerve damage and repair. In: Harris M, Edgar M, Meghji S (eds). Clinical Oral Science. Oxford: Wright, 1998:274–289.
33. Kipp DP, Goldstein BH, Weiss WW Jr. Dysesthesia after mandibular third molar surgery: A retrospective study and analysis of 1,377 surgical procedures. J Am Dent Assoc 1980;100:185–192.
34. Mason DA. Lingual nerve damage following lower third molar surgery. Int J Oral Maxillofac Surg 1988;17: 290–294.
35. Vora AR, Loescher AR, Craig GT, Boissonade FM, Robinson PP. Histological characteristics of human lingual nerve neuromas [abstract]. J Dent Res 2000;79:1192.
36. Bodell SM, Vora AR, Loescher AR, Robinson PP, Boissonade FM. Macrophage accumulation in injured human lingual nerves [abstract]. J Dent Res 2001;80: 1166.
37. Vora AR, Loescher AR, Boissonade FM, Robinson PP. Axonal exposure and close apposition in human lingual nerve neuromas [abstract]. J Dent Res 2003;82:C–564.
38. Mayhew TM. Efficient and unbiased sampling of nerve fibres for estimating fiber number and size. In: Conn PM (ed). Quantitative and Qualitative Microscopy. London: Academic Press, 1990:172–187.
39. Mayhew TM, Sharma AK. Sampling schemes for estimating nerve fibre size. I. Methods for nerve trunks of mixed fascicularity. J Anat 1984;139:45–58.
40. Holland GR. The effect of buffer molarity on the size, shape and sheath thickness of peripheral myelinated nerve fibres. J Anat 1982;135:183–190.
41. Loescher AR, Holland GR. Distribution and morphological characteristics of axons in the periodontal ligament of cat canine teeth and the changes observed after reinnervation. Anat Rec 1991;230:57–72.
42. Friede RL, Beuche W. Combined scatter diagrams of sheath thickness and fibre calibre in human sural nerves: Changes with age and neuropathy. J Neurol Neurosurg Psychiatry 1985;48:749–756.
43. Landon DN. The Peripheral Nerve. London: Chapman & Hall, 1976.
44. Dubner R, Sessle BJ, Storey AT. The Neural Basis of Oral and Facial Function. New York: Plenum Press, 1978.
45. Bunker E, Friede RL. Changes in the histograms of nerves resulting from growth and various modalities of damage. A computer simulation. Acta Neuropathol Berl 1989; 78:521–527.
46. Giannini C, Lais AC, Dyck PJ. Number, size, and class of peripheral nerve fibers regenerating after crush, multiple crush, and graft. Brain Res 1989;500:131–138.
47. Bowe CM, Hildebrand C, Kocsis JD, Waxman SG. Morphological and physiological properties of neurons after long-term axonal regeneration: Observations on chronic and delayed sequelae of peripheral nerve injury. J Neurol Sci 1989;91:259–292.
48. Horch KW, Lisney SJ. On the number and nature of regenerating myelinated axons after lesions of cutaneous nerves in the cat. J Physiol 1981;313:275–286.
49. Schröder JM. Altered ratio between axon diameter and myelin sheath thickness in regenerated nerve fibers. Brain Res 1972;45:49–65.
50. Rushton WAH. A theory of the effects of fibre size in medullated nerve. J Physiol 1951;115:101–122.
51. Shawe GDH. On the number of branches formed by regenerating nerve fibres. Br J Surg 1955;42:474–488.
52. Morris JH, Hudson AR, Weddell G. A study of degeneration and regeneration in the divided rat sciatic nerve based on electron microscopy. II. The development of the "regenerating unit." Z Zellforsch Mikrosk Anat 1972; 124:103–130.

53. Aguayo AJ, Peyronnard JM, Bray GM. A quantitative ultrastructural study of regeneration from isolated proximal stumps of transected unmyelinated nerves. J Neuropathol Exp Neurol 1973;32:256–270.
54. Mathews GJ, Osterholm JL. Painful traumatic neuromas. Surg Clin North Am 1972;52:1313–1324.
55. Carter DA, Lisney SJ. The numbers of unmyelinated and myelinated axons in normal and regenerated rat saphenous nerves. J Neurol Sci 1987;80:163–171.
56. Campbell JN, Raja SN, Meyer RA, Mackinnon SE. Myelinated afferents signal the hyperalgesia associated with nerve injury. Pain 1988;32:89–94.
57. Gautron M, Jazat F, Ratinahirana H, Hauw JJ, Guilbaud G. Alterations in myelinated fibres in the sciatic nerve of rats after constriction: Possible relationships between the presence of abnormal small myelinated fibres and pain-related behaviour. Neurosci Lett 1990;111:28–33.
58. Fried K, Bongenhielm U, Boissonade FM, Robinson PP. Nerve injury-induced pain in the trigeminal system. Neuroscientist 2001;7:155–165.
59. Fried K, Brodin E, Theodorsson E. Substance P-,CGRP- and NPY-immunoreactive nerve fibers in rat sciatic nerve-end neuromas. Regul Pept 1989;25:11–24.
60. Lindqvist A, Rivero-Melian C, Turan I, Fried K. Neuropeptide- and tyrosine hydroxylase-immunoreactive nerve fibers in painful Morton's neuromas. Muscle Nerve 2000;23:1214–1218.
61. Bridges D, Thompson SW, Rice AS. Mechanisms of neuropathic pain. Br J Anaesth 2001;87:12–26.